Computer simulation studies of Ar clusters[†]

P PADMA KUMAR and K J RAO*

Solid State and Structural Chemistry Unit, Indian Institute of Science, Bangalore 560 012, India

Abstract. Results of the solid–liquid transition of Ar_{13} cluster in a spherically symmetric external potential have been presented. The transition temperature is observed to show an elevation with pressure. The broadening of the heat capacity peaks indicate the transition becoming more diffused with pressure. The icosahedral structure of the cluster remains unaltered under pressure. Ar_{55} cluster has also been studied by similar approach. A possible connection between glass transition phenomenon and melting of clusters under pressure has been examined.

Keywords. Computer simulation studies; Ar clusters.

1. Introduction

Discovery of unusual properties of nano-crystalline materials and small atomic clusters has spurred a great interest in the study of small aggregates of atoms and materials in the finely divided state[‡]. Molecular dynamics and Monte Carlo simulation are methods by which properties of small clusters of atoms and molecules can be examined in detail, provided the interaction potentials are known at least fairly accurately (Etters and Kaelberer 1977; Jellinek et al 1986; Davis et al 1987; Labastie and Whetten 1990; Cheng et al 1992; Rose and Berry 1993; Frantz 1995). The unusual stability of isolated clusters of atoms, the magic numbers characterizing stable assemblies and geometries of the resulting aggregation which are often very highly symmetrical but non space filling (Chitra and Yashonath 1996; Häkkinen and Manninen 1996; Ikesyoji et al 1996; Wales 1996; Nayak et al 1997; Sun and Gong 1997), etc are aspects which require to be understood from a fundamental point of view. While free clusters of atoms have been identified experimentally, presence of such clusters in condensed state, with or without requiring a second medium to hold them together are also known. Of particular interest to this work are the clusters held together by a second medium, and are therefore subjected to the pressure exerted by the latter. This situation is often associated with the structure of glasses in which clusters generally possessing a high degree of order of the constituent atoms within themselves are surrounded by an amorphous tissue and are separated

from other similar clusters (Gaskell et al 1979; Bursill 1980). The nature of the pressure exerted by the surrounding tissue can cause both stabilization and deformation of these clusters. The formation of such clusters can be considered as resulting from frustrated growth of the nuclei formed during the nucleation step in supercooled melts. This is either due to enormously high viscosities of the medium or due to stabilization of the surfaces of the clusters due to thermodynamic reasons.

A few salient observations from the published studies on structure, dynamics and thermodynamics—especially the solid–liquid transition of free inert gas clusters are as follows (Etters and Kaelberer 1977; Jellinek et al 1986; Davis et al 1987; Labastie and Whetten 1990; Cheng et al 1992; Rose and Berry 1993): (i) The structures of small inert gas clusters are different from those of the bulk inert gas solids (face centred cubic structure is known to be the most stable in bulk) (Jellinek et al 1986; Davis et al 1987). (ii) The clusters are less stable and boil off at much lower temperatures (e.g. Ar_{13} cluster boils at around 36 K at zero pressure), losing their identity (Etters and Kaelberer 1977). (iii) They show a diffuse solid–liquid transition, which is not first order in the Ehrenfest sense (Etters and Kaelberer 1977; Jellinek et al 1986; Davis et al 1987; Labastie and Whetten 1990). (iv) They exhibit a solid–liquid co-existence (very different from that in the bulk), over a range of temperatures (for Ar_{13}, the range is 29 K–36 K). In this temperature range they keep flipping between solid and liquid phases, as the structural and energetic characterizations reveal (Labastie and Whetten 1990).

The interest in this work is to be able to do computer simulation studies on similar clusters and examine the effect of pressure experienced by the cluster due to the surrounding media on their structures and thermodynamics. Although realistic clusters may consist of

---

hundreds of atoms, we examine here a 13-atom Ar cluster as the first step. We develop a method by which external pressure can be simulated through a plausible and heuristic pressure function. We have extended the method to examine the behaviour of next bigger cluster of 55 Ar atoms. We have used both Monte Carlo (MC) (Allen and Tildesley 1987) and Nose's constant temperature molecular dynamics (NMD) (Nose 1984) methods in the present simulation. Important thermodynamic quantities have been calculated as a function of external pressure. The external pressure has been simulated by the use of a spherically symmetric potential described later. The simulation studies seem to provide some vital clues to the understanding of the phenomenon of glass transition.

2. Simulation studies

2.1 Model potentials

A Lennard–Jones interatomic potential has been used in this simulation and is given by,

$$U^{int} = \sum_{i<j=1}^{N} 4\varepsilon((\sigma/r_{ij})^{12} - (\sigma/r_{ij})^{6}),$$

with $\varepsilon = 120\,k_B$ and $\sigma = 3.4$ Å. The external potential is assumed to have the form,

$$U^{ext} = \sum_{i=1}^{N} A\exp(Br_i^2),$$

where r_i is the distance of ith atom from an initially assigned origin of coordinates, $B = 0.001/\sigma^2$ and A the strength of the external potential, which is varied so as to produce the required external pressure on the system. The above form of external potential is dictated by the fact that the atoms on the surface experience a much higher force than those near the centre. The external and internal pressures, P^{ext} and P^{int} respectively, are defined as follows (Allen and Tildesley 1987),

$$P^{ext} = \sum_{i=1}^{N} \mathbf{r}_i \cdot \mathbf{F}_i^{ext}/V,$$

where $\mathbf{F}_i^{ext}$ is the external force on the ith particle.

$$P^{int} = W/V + (3N - 6)k_B T/V,$$

where, $W = \sum_{i<j=1}^{N} \mathbf{r}_{ij} \cdot \mathbf{F}_{ij}/3,$

is the virial, N, the number of particles in the system, k_B, the Boltzmann constant, $\mathbf{F}_{ij}$, the force on ith particle due to the jth and $\mathbf{r}_{ij} = \mathbf{r}_i - \mathbf{r}_j$, where $\mathbf{r}_i$ and $\mathbf{r}_j$ are the position vectors to the ith and jth particles from the origin. T is

the temperature (instantaneous temperature in molecular dynamics (MD) and the temperature at which the sampling is done in the case of Monte Carlo (MC)). The time (or ensemble) averaged $\langle P^{ext}\rangle$ and $\langle P^{int}\rangle$ are expected to be equal at equilibrium.

Definition of cluster volume used in the expression for pressure is a major problem in these studies. This is due to the fact that the surfaces of small clusters are rather rough in comparison to their dimensions and use of continuum approximation to calculate their volumes is of doubtful validity. As a consequence the definition of pressures also becomes ambiguous. However, the instantaneous volume, V of the cluster is defined following Cheng *et al* (1992) as

$$V = \frac{4\pi}{3}(d/2)^3,$$

where d is the largest value of the centre to centre separation of atoms in the cluster. We have tried to evaluate the appropriateness of this definition later, by comparing $\langle P^{int}\rangle$ and $\langle P^{ext}\rangle$ of the clusters, at various values of $\langle P^{ext}\rangle$ for different temperatures.

The total Hamiltonian of the system is therefore given as,

$$H^{sys} = \sum_{i=1}^{N} \frac{p_i^2}{2m} + U^{int} + U^{ext}.$$

Extensive MC simulation (Allen and Tildesley 1987), has been performed over a wide range of temperatures (5 K–95 K) and pressures (20 atm.–1000 atm.). Nose's (1984) constant temperature molecular dynamics has also been performed over a smaller range of temperatures and pressures—mainly to check the correctness of results.
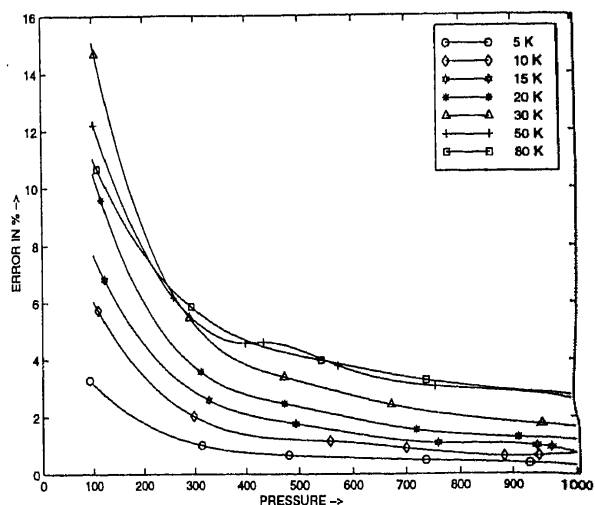

Figure 1. ΔP values as a function of $\langle P^{ext}\rangle$ (in atm.) for a few temperatures, for Ar_{13}. Symbols represent actual data points and continuous lines are spline fits.

Both the methods give canonical ensemble averages. The methods themselves are briefly described below.

(I) *The MC method*: The standard Metropolis method (Allen and Tildesley 1987) has been used with slight modifications in order to include the effect of the external potential on the system. The transition probability between states n and $n + 1$ in this case is given by,

$$W_{n,n+1} = \exp[-\beta(U_{n+1}^{\text{tot}} - U_n^{\text{tot}})],$$

where, $U_n^{\text{tot}} = U_n^{\text{int}} + U_n^{\text{ext}}$ and $\beta = 1/k_B T$.

The new state $n + 1$ is accepted if, $W_{n,n+1} \geq \xi$ or rejected if, $W_{n,n+1} < \xi$, where ξ is a random number between zero and one.

(II) *The Nose's MD method*: Nose's method makes use of an extended Hamiltonian given by,

$$H^{\text{extd}} = \sum_{i=1}^{N} \frac{p_i^2}{2ms^2} + U^{\text{tot}} + \frac{p_s^2}{2Q} + (3N - 5) k_B T \ln s,$$

where Q and s may be interpreted as the mass and coordinate of the pseudo particle, which exchanges energy with the particles in the system. It has been shown that the MD (micro-canonical ensemble) average of any quantity given by the H^{extd} is precisely the same as the canonical ensemble average given by H^{sys} (Nose 1984). Also this extended Hamiltonian assures an average temperature $\langle T \rangle$ numerically equal to the required (input) temperature, T. In the present study, Q was kept equal to $10 \, \sigma^2$ amu throughout.
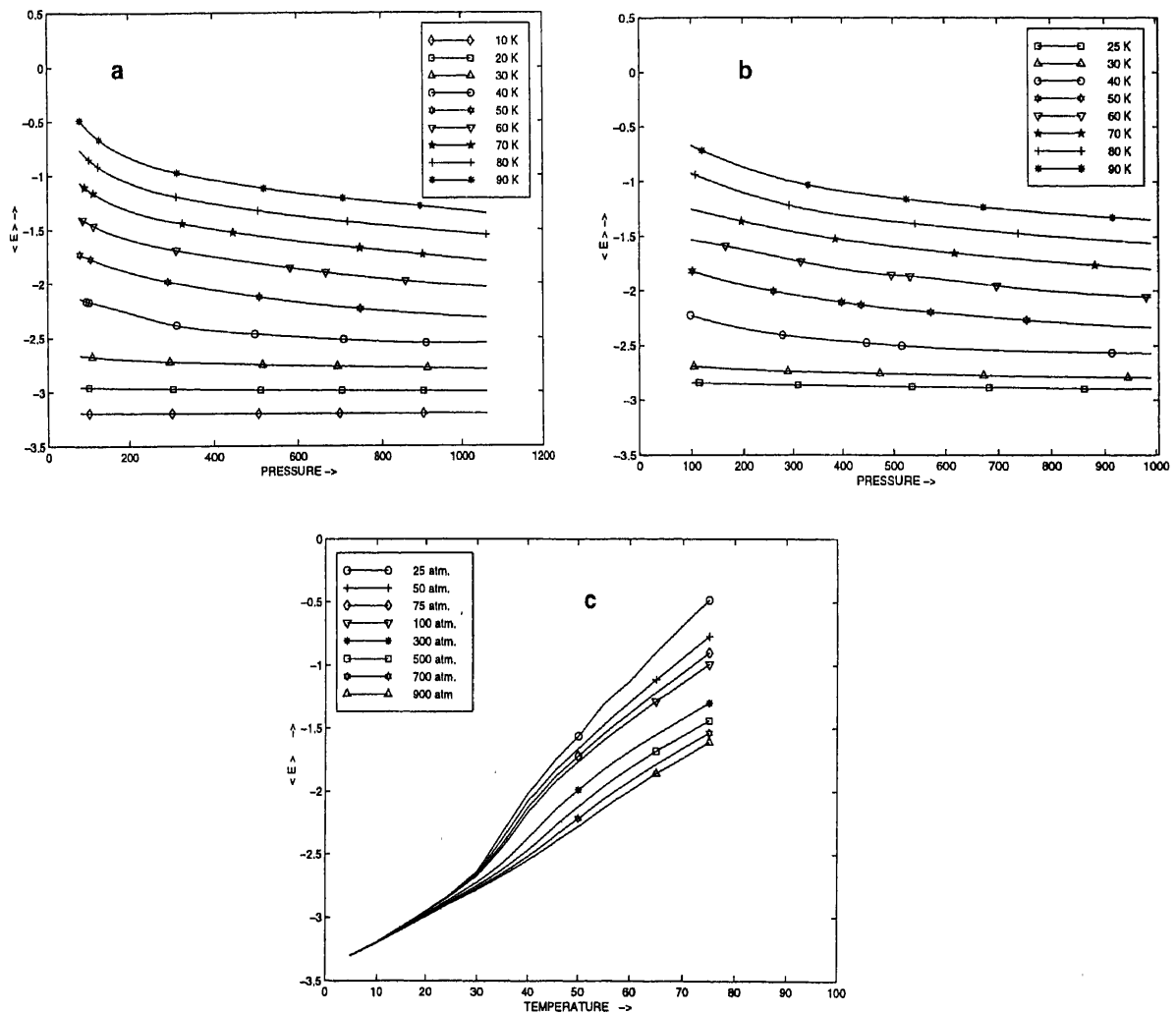

Figure 2. The average total internal energy (per atom, in units of ε) isotherms as a function of $\langle P^{\text{ext}} \rangle$ (in atm.) (a) from MC; (b) from NMD and (c) internal energy isobars generated from (a) as a function of temperature (in K), for Ar_{13}. Symbols in (a) and (b) represent simulation data. Symbols in (c) are only to identify the curves.

2.2 *Details of simulation runs*

For the NMD studies we have used the algorithm suggested by Fox and Andersen (1984). We have chosen a time increment of ~ 3 fs. Nearly 10^6 steps were devoted for adjusting the parameter A, in the external pressure function in order to produce the required pressure on the system. The value of A is held constant thereafter. The system is then equilibrated for further 2×10^6 steps, and averages are calculated for another 10^7 steps. In the MC calculation also 10^6 steps were devoted for pressure adjustment, 2×10^6 steps for equilibration and 5×10^6 steps for property averaging. Even then the present method does not offer good control of pressure on the system. Hence isotherms were generated (for average total internal energy, heat capacity and root mean square bond length fluctuation), at various temperatures. These isotherms were interpolated at required pressures, and

isobars at various pressures were generated. Matlab (version 5.0.0.4064) cubic spline interpolation function was used for the above purpose. Simulation runs were carried out on IBM/580 work stations.

3. Results and discussion

The limitations arising from the definition of volume was first examined by calculating ΔP, from NMD, which is defined as,

$$\Delta P = \frac{\left\langle P^{\text{int}} \right\rangle - \left\langle P^{\text{ext}} \right\rangle}{\left\langle P^{\text{int}} \right\rangle} \times 100.$$

In figure 1, ΔP is plotted as a function of pressure at various temperatures. The observed discrepancy in the calculated $\langle P^{\text{int}} \rangle$ and $\langle P^{\text{ext}} \rangle$ can be attributed to the
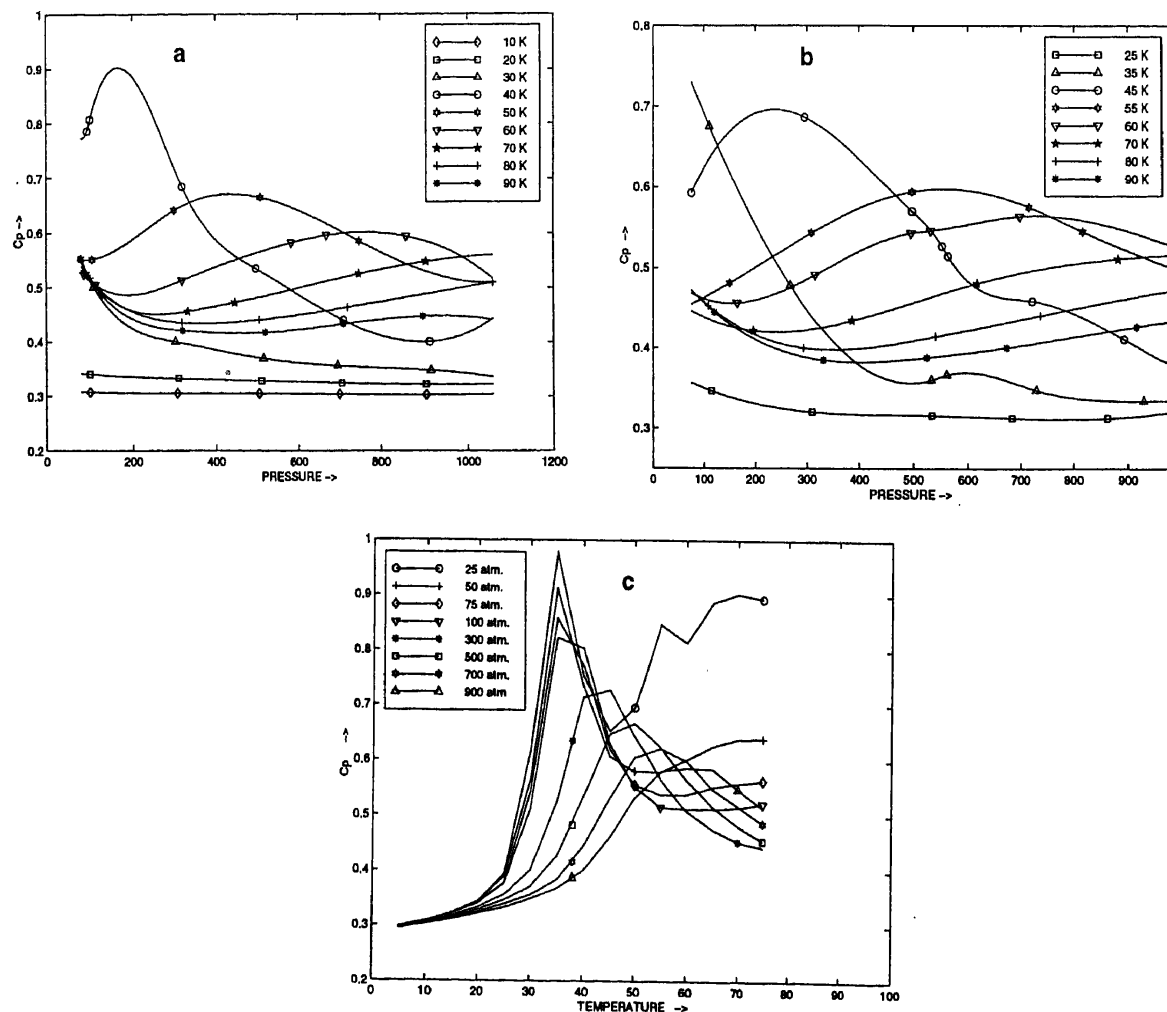

Figure 3. Heat capacity (in ε K^{-1} units) isotherms as a function of $\langle P^{\text{ext}} \rangle$ (in atm.) (a) from MC; (b) from NMD and (c) heat capacity isobars generated from (a) as a function of temperature (in K), for Ar$_{13}$. Symbols in (a) and (b) represent simulation data. Symbols in (c) are only to identify the curves.

inadequate definition of volume. Though, ΔP keeps increasing with temperature, it decreases with increasing $\langle P^{ext}\rangle$, which is encouraging. Since P^{ext} is not used directly in the subsequent calculations, we consider it as sufficiently accurate for examining the influence of external force on the cluster properties.

The total internal energy (the average value of H^{sys}) isotherms from MC and NMD are shown in figures 2a and 2b. The isobars generated from figure 2a are shown in figure 2c. The heat capacities (C_P) were calculated from the total energy fluctuations as,

$$C_P = \frac{\left\langle U^{tot^2}\right\rangle - \left\langle U^{tot}\right\rangle^2}{k_B T^2}.$$

The comparisons of heat capacity isotherms shown in figure 3a (from MC) and figure 3b (from NMD) also reveal good agreement. As the pressure is increased the peak-heights lower and peak-widths broaden as seen in figure 3c (the C_P isobars are generated from figure 3a). This is a clear indication that the transition becomes more and more diffuse and smeared with increasing pressure. The shifts of the peaks also reveal that the solid–liquid (SL) transition temperature, T_t increases with pressure.

The root mean square bond length fluctuation δ, is a very useful quantity to locate solid–liquid transition temperature, T_t (Etters and Kaelberer 1977; Jellinek *et al* 1986; Davis *et al* 1987). δ is defined as,
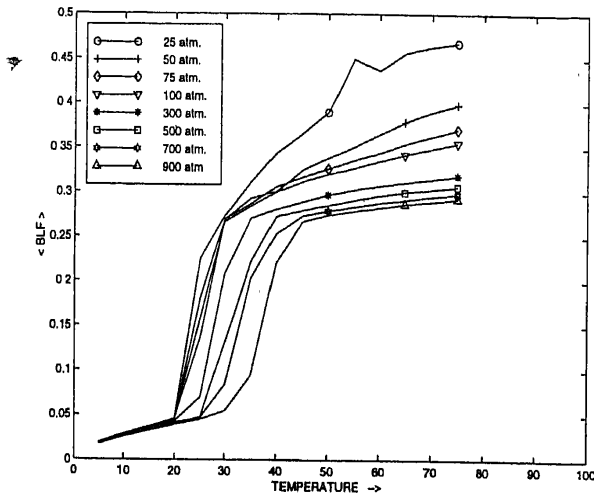

Figure 4. Average root mean square bond length fluctuation ($\langle$BLF$\rangle$) as a function of temperature for various pressures (in atm.), for Ar$_{13}$. Symbols are only to identify the curves.
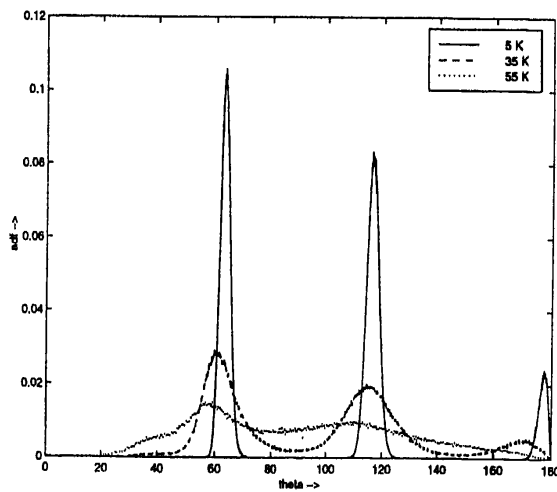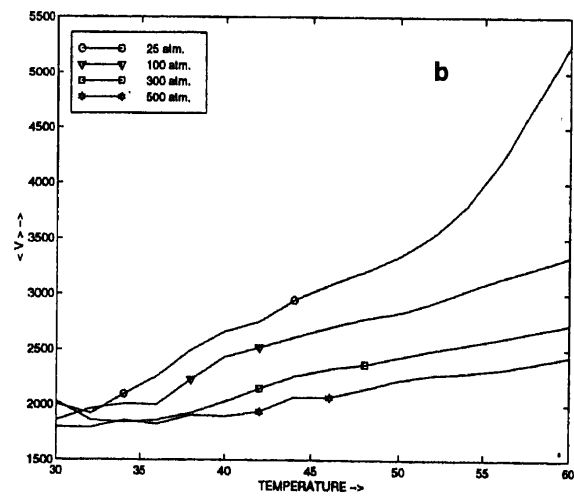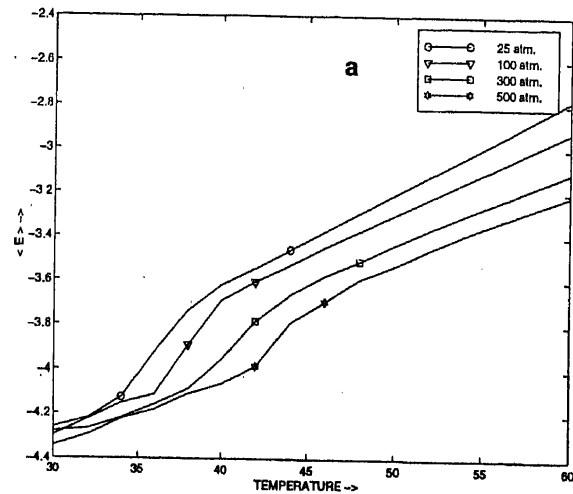

Figure 5. Angle distribution functions at 5 K, 35 K and 55 K at about 100 atm.

Figure 6. (a) The average total internal energy per atom (in units of ε) and (b) average volume (in Å^3) as a function of temperature (in K) for various $\langle P^{ext}\rangle$ values for Ar$_{55}$. Symbols are only to identify the curves.

$$\delta = \frac{2}{N(N-1)} \sum_{i<j=1}^{N} \frac{\sqrt{\langle r_{ij}^2 \rangle - \langle r_{ij} \rangle^2}}{\langle r_{ij} \rangle}.$$

δ exhibits a sharp change from 0·1 to 0·3, in a narrow temperature range, around T_t as shown in figure 4. When $\delta \le 0·1$ it corresponds to a purely solid phase (so called Lindemann criterion) and when $\delta \ge 0·3$ it represents a purely liquid phase. The temperature range in which δ rises rapidly from 0·1 to 0·3 marks the co-existence of solid and liquid phases. It may be noted that δ is quite easy to calculate in simulation studies and its behaviour is somewhat insensitive to the details of the interaction potential. The δ calculated as a function of temperature at various pressures confirms that the peaks observed in C_P plots (figure 3c), indeed, correspond to the melting of the cluster and not to any solid–solid structural transition. It can be seen that δ tends to flatten out at values less than 0·3,·at high pressures.

At low pressures (e.g. 25 atm. and 50 atm.) and at high temperatures (above 50 K), yet another C_P peak (though very broad) emerges (figure 3c). This is most likely due to the onset of liquid–gas transition of the cluster. Near liquid–gas transition a sharp change in δ has been reported in 2D systems by Rivera *et al* (1995). But we have not observed a sharp change of δ in this region.

Figure 5 shows the angle distribution function (ADF), calculated with respect to the central atom, using all triplets of atoms in the cluster for three different temperatures at about 100 atm. pressure. There are peaks observed in ADF at 60°, 120° and 180° and they correspond to the angles expected to be present in an icosahedral structure (Davis *et al* 1987). The application of isotropic pressure, therefore, appear to leave the icosa-

hedral structure of the Ar_{13} cluster largely unaffected, till the melting temperature.

3.1 *The 55-atom Ar cluster*

Using the same interaction potential as employed for the 13-atom cluster, MC calculations were performed for a 55-atom argon cluster (Ar_{55}). The energies were computed for 15×10^6 steps in the transition region. The number of steps were reduced to 5×10^6 in the post transition region. Average energies, average volumes (figures 6a and 6b, respectively) and heat capacities (figure 7) were evaluated at various pressures (from 25 atm. to 500 atm.) as a function of temperature. The heat capacity variations are shown only for a few pressures for the sake of clarity. It may be noted that variation of energy, volume and heat capacities is qualitatively similar to the variation of the same quantities for Ar_{13} cluster. The volume behaviour at 25 atm. pressure is also suggestive of the liquid–vapour transition around 55 K. The solid–liquid co-existence region and the bond length fluctuation behaviour are also similar for Ar_{55} cluster (figure 8).

Most important for the present discussion is the behaviour of heat capacities of the cluster for the various pressures. Although the peak heights seem to exhibit a slight increase at lower pressures, their heights decrease and the peaks broaden out at higher pressures. The heat capacity peaks shift to higher temperatures as the pressure is increased.

The transition temperature noted from the C_P peaks as a function of pressure, for Ar_{13} and Ar_{55} clusters, are shown in figure 9. At higher pressures the transition temperature of the Ar_{55} cluster is somewhat lower than that of Ar_{13} cluster. Also, the pressure coefficient of the transition temperature is slightly lower for the bigger cluster.
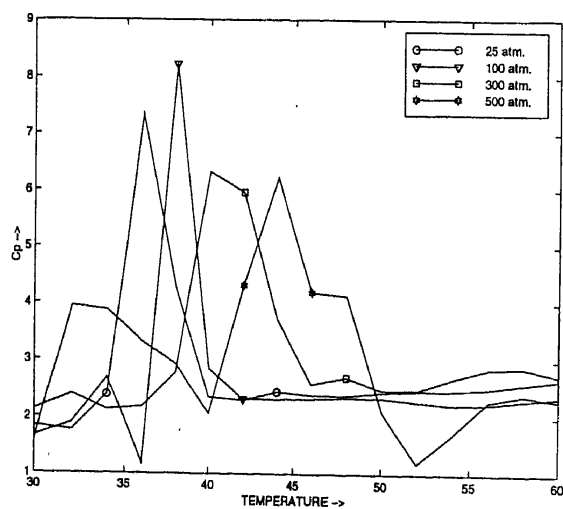

Figure 7. Heat capacity (in ε K^{-1} units) isobars as a function of temperature (in K) for Ar_{55}. Symbols are only to identify the curves.
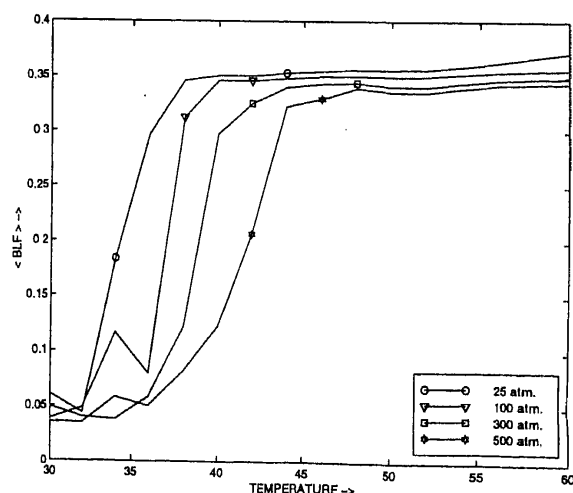
Figure 8. Average root mean square bond length fluctuation ($\langle BLF \rangle$) as a function of temperature (in K) for various $\langle P^{ext} \rangle$ values for Ar_{55}. Symbols are only to identify the curves.

The compressibilities of the Ar_{13} and Ar_{55} clusters calculated from the volume fluctuations (Allen and Tildesley 1987) are $156 \times 10^{-11}\, m^2 N^{-1}$ and $4942 \times 10^{-11}\, m^2 N^{-1}$ (at 5 K and 25 atm.) respectively. This may be compared to the experimental compressibility of bulk argon $98.8 \times 10^{-11}\, m^2 N^{-1}$ (at 10 K and 0 atm.) (Dobbs and Jones 1957). Although the compressibility of Ar_{55} cluster is significantly higher than that of Ar_{13}, it is still surprising that the compressibilities of simulated clusters reflect reasonable magnitudes.

3.2 Relevance to the glass transition phenomenon

Cluster models of glass transition (Rao and Rao 1982; Parthasarathy et al 1983; Rao 1984) assume that glasses possess a cluster tissue texture, with clusters held in a matrix of the tissue. These clusters are generally assumed to be characterized by a greater topological order compared to that of the tissue, which is truly amorphous. The ordered arrangement of constituents in clusters has been evidenced in several lattice imaging studies (Gaskell et al 1979; Bursill et al 1980). These clusters generally are of the dimensions of several angstroms and therefore consist of several hundred atoms. It is possible in glasses where lattice fringes have not been observed in electron microscopic studies that the clusters are much smaller. The point of interest in this work is that in real glasses, clusters are subjected to the high pressures exerted by the surrounding amorphous matrix of the tissue.

The cluster model considers the glass transition as corresponding to the melting of the clusters, but they melt after the tissue itself melts. Since small clusters melt at characteristically lower temperatures, it would be more realistic to assume that clusters melt first and then the surrounding tissue dissolves into the molten clusters. In such a situation we should expect the variation of heat capacities of glasses to be dominated by the heat capacity variations of the clusters. Indeed the heat capacity behaviour during the melting of Ar_{13} cluster shown in figure 3c is highly reminiscent of variations of heat capacity around T_g of most real glasses. We should therefore like to examine on a heuristic basis the implications of the pressure dependence of heat capacities of clusters to a possible origin of the glass transition in materials.

The Ar_{13} cluster has a volume of $506.9\, Å^3$ (at 5 K and 25 atm.). In the bulk argon, volume occupied by 13 atoms of Ar is $486.59\, Å^3$ (at 0 K and 0 atm.). In a hypothetical argon glass therefore a 13-atom cluster would have been subjected to a pressure by the matrix, whose magnitude is such that the cluster volume has decreased to its characteristic bulk volume. On the basis of the compressibility of Ar_{13} cluster, the pressure due to the matrix can be estimated as 267.2 atm (at 5 K). But at such an external pressure (267.2 atm.), the Ar_{13} cluster is expected
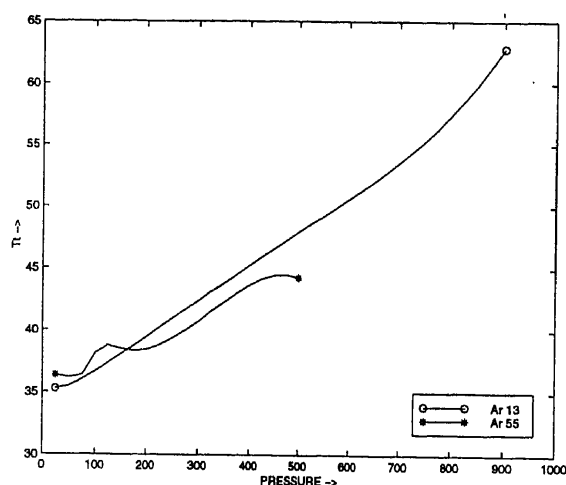

Figure 9. Melting points (in K) of Ar_{13} and Ar_{55} as a function of $\langle P^{ext} \rangle$ (in atm.). Symbols are only to identify the curves.

to melt at an elevated temperatures of about 42 K (interpolated value from figure 9). The hypothetical argon glass should therefore exhibit a glass transition at 42 K, and give rise to the typical C_P behaviour shown in figure 3c. Indeed 42 K is equal to $0.5\, T_m$, where T_m is the melting point (84 K) of solid argon. Thus $T_g/T_m \approx 0.5$, for the hypothetical glassy argon (Angell 1981). The value is suggestive of why argon does not form a glass easily. The compressibility of Ar_{55} cluster is somewhat anomalous and therefore a similar estimate of T_g was not attempted. This study therefore suggests that in all real glasses, the existence of a cluster–tissue texture with cluster volumes of the order of a few Å in radius are likely to be subjected to pressure in the range of a few 100 atmospheres, and their melting under pressure manifests as glass transition. This approach needs further examination by simulation studies on glass forming materials like SiO_2.

Acknowledgements

References

Allen M P and Tildesley D J 1987 *Computer simulation of liquids* (Oxford: Oxford University Press)

Angell C A 1981 in *Annals of the New York Academy of Sciences* (eds) J M O'Reilly and M Goldstein 371 p. 136

Bursill L, Thomas J M and Rao K J 1980 *Nature* **289** 157

Cheng Hai-Ping, Li Xiuling, Whetten R L and Berry R S 1992 *Phys. Rev.* **A46** 791

Chitra R and Yashonath S 1996 *Chem. Phys. Letts* **252** 384

Davis H L, Jellinek J and Berry R S 1987 *J. Chem. Phys.* **86** 6456

Dobbs E R and Jones G O 1957 *Rep. Prog. Phys.* **20** 516

Etters R D and Kaelberer J 1977 *J. Chem. Phys.* **66** 5112

Frantz D D 1995 *J. Chem. Phys.* **102** 3747

Fox J R and Andersen H C 1984 *J. Phys. Chem.* **88** 4019

Gaskell P H, Smith D J, Catto C J D and Cleaver J R A 1979 *Nature* **281** 465

Häkkinen H and Manninen M 1996 *Phys. Rev. Letts* **76** 1599

Ikesyoji Tamio, Hafskjold Bjørn, Hashi Yuichi and Kawazoe Yoshiyuki 1996 *J. Chem. Phys.* **22** 5126

Jellinek J, Beck T L and Berry R S 1986 *J. Chem. Phys.* **84** 2783

Labastie P and Whetten R L 1990 *Phys. Rev. Letts* **65** 1567

Nayak S K, Jena P, Stepanyuk V S, Hergert W and Wildberger K 1997 *Phys. Rev.* **B56** 6952

Nose S 1984 *Mol. Phys.* **52** 255

Parthasarathy R, Rao K J and Rao C N R 1983 *Chem. Soc. Rev.* **12** 361

Rao K J 1984 *Proc. Indian Acad. Sci. (Chem. Sci.)* **93** 389

Rao K J and Rao C N R 1982 *Mater. Res. Bull.* **17** 1337

Rivera Y, Weber D C and Lopez G E 1995 *J. Chem. Phys.* **103** 10627

Rose J P and Berry R S 1993 *J. Chem. Phys.* **98** 3246

Sun D Y and Gong X G 1997 *J. Phys.: Cond. Matter* **9** 10555

Wales D J 1996 *Science* **271** 925